COB-2019-0240
DYNAMICAL ANALYSIS OF A DRILL-STRING WITH LATERAL-TORSIONAL COUPLING

Frederico Dias Souza
Universidade Federal do Rio de Janeiro, Centro de Tecnologia - CEP 21941-909, Rio de Janeiro, RJ
fredericods@poli.ufrj.br
Thiago Gamboa Ritto
Universidade Federal do Rio de Janeiro, Centro de Tecnologia - CEP 21941-909, Rio de Janeiro, RJ
tritto@mecanica.ufrj.br
Romulo Reis Aguiar
Brazil Technology Integration Center - Schlumberger Oilfield Services, Rio de Janeiro, RJ
RAguiar@slb.com

Abstract. *Problems arising from vibrations while drilling represent a high cost to the oil industry, so it is indispensable the development of dynamic drilling models that can predict these vibrations. In this paper, we propose a simplified three degree of freedom dynamical model able to simulate the main phenomena related to oil well drilling. The model consists of a torsional pendulum coupled with a Jeffcott rotor. We analyzed different rotational speeds under three conditions: lateral formulation, lateral-torsional without stick-slip and lateral-torsional with stick-slip. From the results, it is possible to verify the operational conditions that lead to these vibrations, and also how these parameters influence time responses.*

Keywords: *Dynamical Analysis, Drill-string, Well drilling, Forward Whirl, Stick-slip*

1. INTRODUCTION

Oil well drilling is one of the most important and complex activities in oil and gas industry and can represent up to 40% of the exploration and development costs of a well according to (Cunha, 2002). The occurrence of undesirable vibrations is intrinsic to the drilling process. The vibrations can be divided into three types: axial, torsional and lateral.

Axial vibrations, in severe situations, are commonly associated with damage to the drilling bit and may cause bit bounce, the repeated impact of the bit with bottomhole. While severe torsional vibrations can cause irregular rotation at the bottomhole, called stick-slip, that is the fluctuation of the rotational speed of the bottomhole assembly (BHA) (Brett *et al.*, 1992).

Finally, lateral vibrations may lead to two kinds of whirl: forward and backward. Forward whirl is generally caused by the imbalance on the assembly and can cause the uneven wear of the drill-string. The contact between the drill pipes and the well may excite backward whirl. This is the most severe form of vibration, resulting in strong fatigue (Butlin and Langley, 2015).

Problems arising from vibrations represent a high cost to the oil industry, due to the wide range of problematic phenomena. As stated by (Wu *et al.*, 2012), in deepwater drilling, low productivity associated with vibrations can significantly impair a project profitability. The same work claims that more than 40% of the drilled length around the world is affected by whirl of the drill-string and the occurrence of stick-slip corresponds to about 50% of the drilling time.

That way, according to (Butlin and Langley, 2015), there is a need for dynamic models of drill-strings that are able to predict this variety of phenomena, efficient enough to perform parametric studies and simple to allow understanding the physics underlying the operation.

Given the importance of studying such vibrations, this work aims at: i. proposing a model with three degrees of freedom that is able to simulate the stick-slip and the forward whirl; ii: analyzing the coupling between lateral and torsional vibrations and; iii: analyzing the influence of operating parameters on the occurrence of typical vibrational phenomena. It is worth mentioning that axial vibrations are not taken into account.

2. PHYSICAL MODEL

In order to simulate the stick-slip, the string was modeled as a simple torsional pendulum of one degree of freedom, with the drilling bit acting under a regime of dry friction, that is, does not consider the existence of fluid between the bit and the well bottom. This is the same approach proposed by (Navarro-López and Suárez, 2004), widely used for the simulation of the torsional behavior of a drill-string.

The whirls are governed by the rotodynamic equations of two degrees of freedom. The forward whirl arises from the imbalance of the rotor in relation to the center of mass, intrinsic to Jeffcott rotor (Ishida and Yamamoto, 2013).

For the coupling of the three degrees of freedom, it was considered for the Jeffcot rotor that its angular acceleration was different from zero. Hence, the angular speed $\dot{\theta}$ and angular acceleration $\ddot{\theta}$ imposed on the rotodynamic model are calculated from the torsional formulation. Thus, the torsional model influences the lateral, but is not affected by it.

The three degrees of freedom model are represented by the union of the torsional pendulum with the Jeffcott rotor, as shown in Figure 1 and described by the system of Equations (1) and (2).

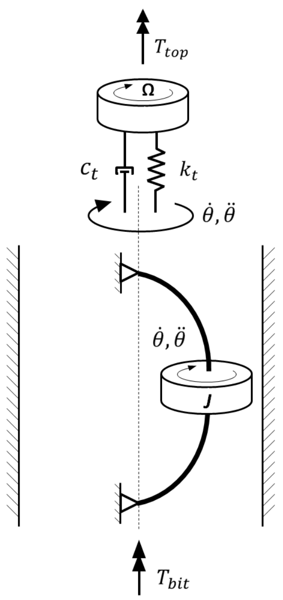

Figure 1. 3 DOF model: Torsional Pendulum and Jeffcott Rotor

$$J\ddot{\theta}(t) + c_t\dot{\theta}(t) + k_t\theta(t) = c_t\Omega + k_t\Omega t - T_{bit} \quad (1)$$

$$\begin{aligned} m\ddot{x}(t) + c\dot{x}(t) + kx(t) &= me\dot{\theta}^2 cos(\dot{\theta}t) + me\ddot{\theta} sen(\dot{\theta}t) \\ m\ddot{y}(t) + c\dot{y}(t) + ky(t) &= me\dot{\theta}^2 sen(\dot{\theta}t) - me\ddot{\theta} cos(\dot{\theta}t) \end{aligned} \quad (2)$$

The Equation (1) corresponds to the torsional pendulum, rotated by the top drive at a prescribed constant speed Ω. The drill-string, which angular position is expressed by θ, can be interpreted as a torsional spring of inertia J, stiffness k_t and damping c_t, that connects the top drive to the drilling bit. According to (Kyllingstad *et al.*, 1987), the string inertia can be expressed from the drill pipes inertia and BHA inertia, as shown by Eq. 3.

$$J = \frac{1}{3}J_{dp} + J_{bha} \quad (3)$$

As prescribed speed is constant, from the equilibrium of body at the top of Figure 1, the top drive torque T_{top} is given by Eq. 4.

$$T_{top}(t) = c_t(\Omega - \theta) + k_t(\Omega t - \dot{\theta}) \quad (4)$$

Besides, as stated by (Tucker and Wang, 1997), the torque on bit T_{bit} is described by Eq. 5, with some adaptations to provide dimensional coherence. It is a function dependent on the angular speed $\dot{\theta}$ and weight on bit WOB, where r_{bit} is drilling bit ray, ψ the coefficient of interaction between the bit and the rock, and α_0, α_1 and α_2 are related to the rock properties. The curve was adjusted to follow the behavior of the experimental data presented in (Ritto *et al.*, 2017).

$$T_{bit}(WOB, \dot{\theta}) = r_{bit}\psi WOB \left(tanh\, \alpha_0\dot{\theta} + \frac{\alpha_1\dot{\theta}}{1 + \alpha_2\dot{\theta}^2} \right) \quad (5)$$

Regarding the rotodynamic formulation expressed by Eqs. (2), (Jeffcott, 1919) proposed a dynamic model for rotary machines, which consisted of a negligible mass axis supported by rigid bearings, with a rigid disk with mass *m* mounted in the middle of its length, rotating at speed $\dot{\theta}$ and acceleration $\ddot{\theta}$. The center of rotation or geometric center of the disk *C* and its center of mass *CM* are offset by a distance *e*, called static displacement. The shaft limits the disc movement by a lateral stiffness *k* and damping *c*.

Figure 2 illustrates the analogy between the Jeffcott rotor and the drill-string. The stabilizers acts as the rigid bearings and only the BHA region between them are considered on lateral dynamics. For the model adopted, we considered that the mass *m* only is the total mass of the region between the stabilizers, different from the torsional model, which takes into account the entire column.

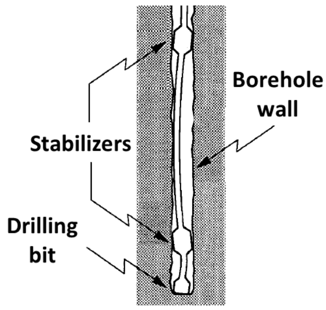

Figure 2. Drill-string whirl. Adapted from Jansen *et al.* (1992).

3. RESULTS AND DISCUSSION

The results presented in this section are governed by the Eqs. (1) and (2). Defining the system lateral stiffness as $k = 490745N/m$ and mass $m = 4672kg$, lateral natural frequency is approximately 100 rpm. At this extend abstract, we analyse the results for the rotational speeds 50 rpm, 100 rpm and 200 rpm.

As torque on bit T_{bit} depends on the weight on the bit *WOB* and the drilling bit rotation $\dot{\theta}$, the operating regime is described as a function of these two parameters. For instance, in case of low bit rotation and high weight on bit, the stick-slip is more likely to happen, that is, the bit rotation oscillates permanently, even the top drive rotation Ω being constant. In case of high rotational speed and low weight on bit, the stick-slip does not occur and the bit rotation tends to the constant value Ω.

This way, we analyse the results of lateral formulation in three situations: i. constant rotation, that is, when the system in only governed by Jeffcott Rotor, Eq. (2); ii: rotation without stick-slip; iii: rotation in case of stick-slip. On Figure 3, we see the results when the rotational speed is abot half of natural frequency, 50 rpm. It is possible to see the $\dot{\theta}$ and radius amplitude time responses for each of these three cases. The radius amplitude corresponds to the distance between the geometric center *C* of Jeffcott disk and the center of the borehole.

For the case without stick-slip, the transient stretches considerably, but the steady state does not change, still tending to the steady state radius of the lateral formulation. In the case with stick-slip, the response changes considerably, assuming an oscillatory format permanently. Thus, the stick-slip does not potentiate fatigue only in the torsional direction, but also in the lateral.

Figure 4, which shows the radius time response of the radius for a time window of 1000s, allows a better understanding of this stick-slip behavior. The amplitude decreases continuously and remains almost constant between 950s and 1000s, as shown in Figure 5, still not reaching its steady state. It is important to note that the response reaches lower amplitudes than those in steady regime of the cases without stick-slip.

Regarding the orbits, Figure 6 shows that, for the case without stick-slip, the orbit of the geometric center of Jeffcott disk assumes a constant whirl radius in the steady state. The red arrows indicate that the whirl direction. As for the situation with stick-slip, Figure 7, the orbit changes completely in relation to the case of constant speed, ceasing to be a circular trajectory. In this case, due to its atypical shape, it is difficult to detect the whirl direction.

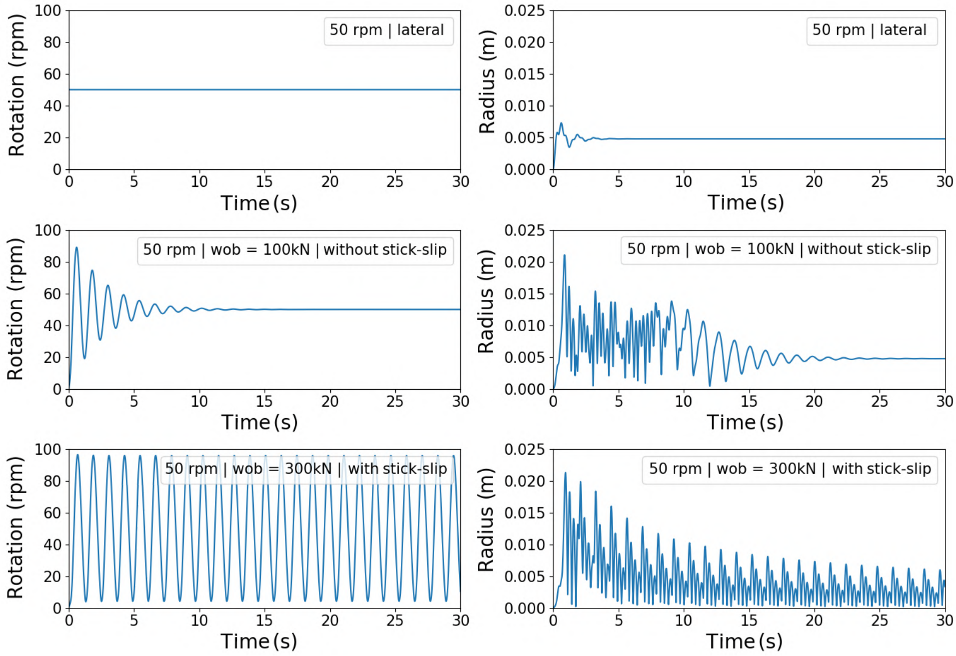

Figure 3. Influence of the coupling on radius time response ($\Omega = 50rpm$)

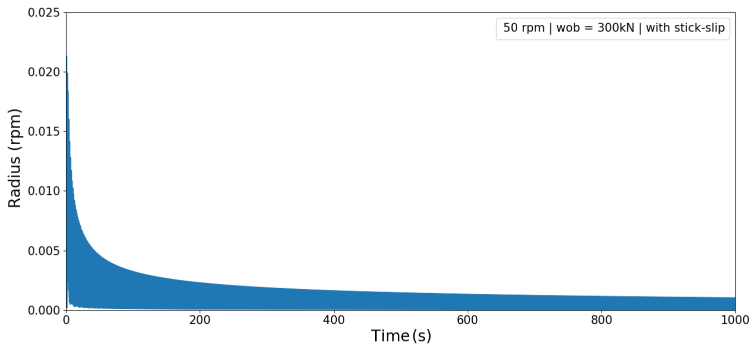

Figure 4. Radius Time Response for $\Omega = 50rpm$ and stick-slip

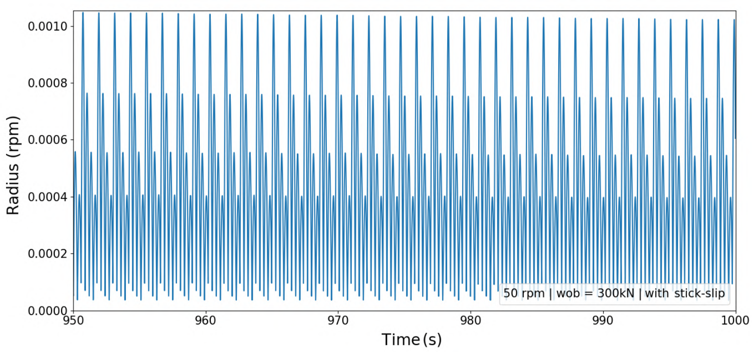

Figure 5. Radius Time Response for $\Omega = 50rpm$ and stick-slip between 950s and 1000s

As shown in Figure 8, all these behaviors are maintained for when the top-drive rotational corresponds to 200 rpm: in the case without stick-slip, only the transient changes, whereas in the case with stick-slip, the response maintains its oscillatory behavior permanently. It is worth mentioning that there is a prominent peak between 7s and 10s for the case without stick-slip, most probably because the spin passes about three times at natural frequency, leading to this increase in amplitude.

The orbits for 200 rpm are shown in Figure 9 - without stick-slip - and Figure 10 - with stick-slip and exhibit a behavior similar to the previous case, at 50 rpm.

When top-drive rotational speed approaches the natural frequency, the behavior changes, as shown in Figure 11. For

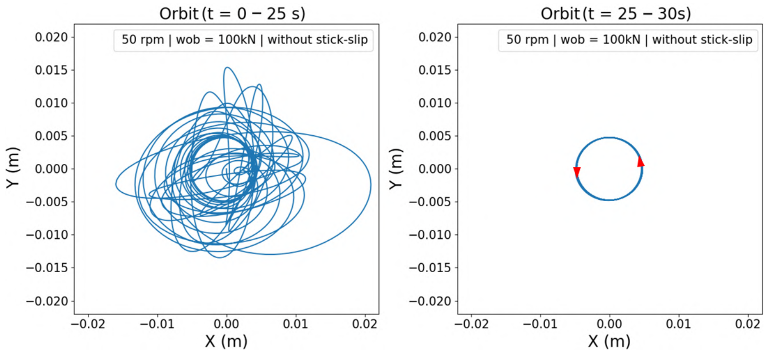

Figure 6. Orbit without *stick-slip* ($\Omega = 50rpm$)

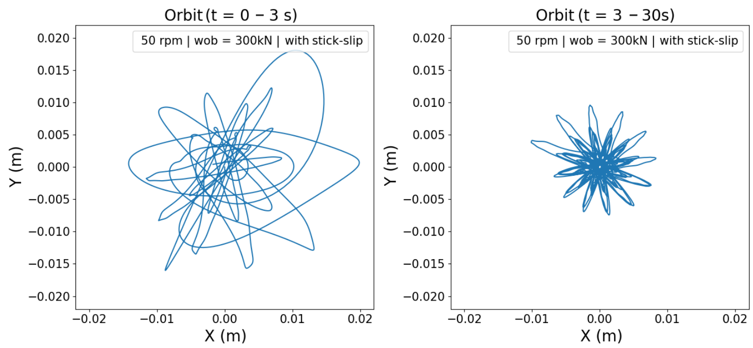

Figure 7. Orbit with *stick-slip* ($\Omega = 50rpm$)

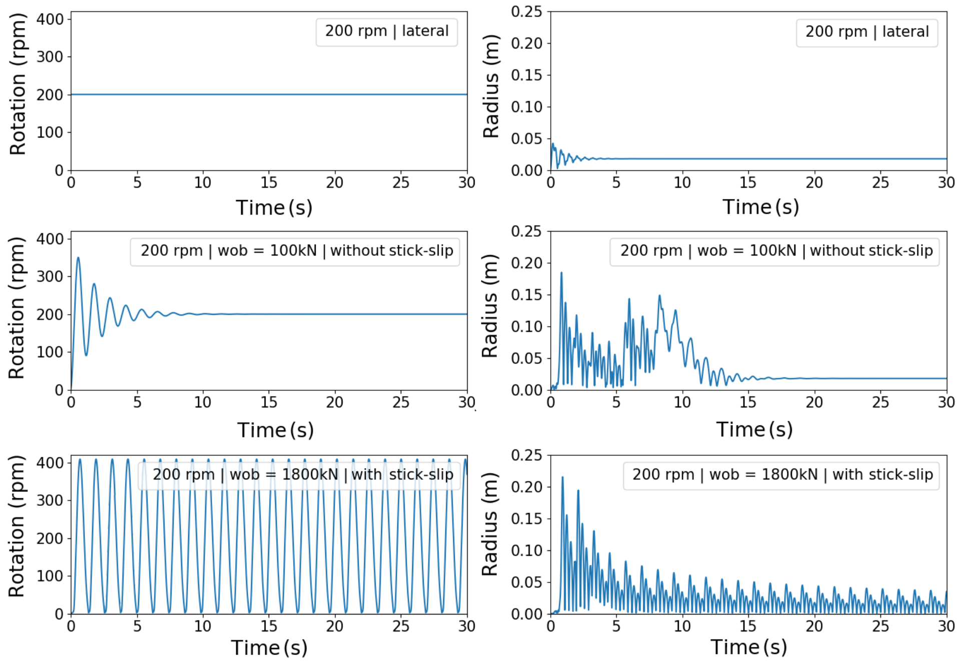

Figure 8. Influence of the coupling on radius time response ($\Omega = 200rpm$)

the stick-slip case, the response does not oscillate around the steady-state radius. Since the rotational speed only passes through the natural frequency, the system does not resonate. In this sense, the stick-slip ends up being beneficial to the deflection of the column. As for the case without stick-slip, the response behaves in a similar way to other cases, with the introduction of a more oscillatory and long transient.

Finally, the orbits for 100 rpm are shown in Figure 12 - without stick-slip - and Figure 13 - with stick-slip. The comparison between them allows to better visualize how much the amplitude in the case with stick-slip is considerably smaller than the without stick-slip.

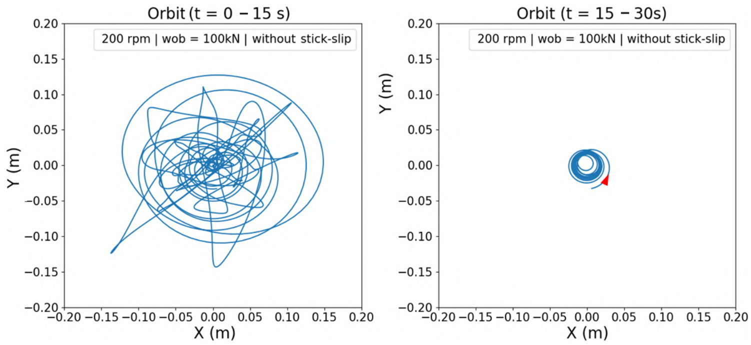

Figure 9. Orbit without *stick-slip* ($\Omega = 200rpm$)

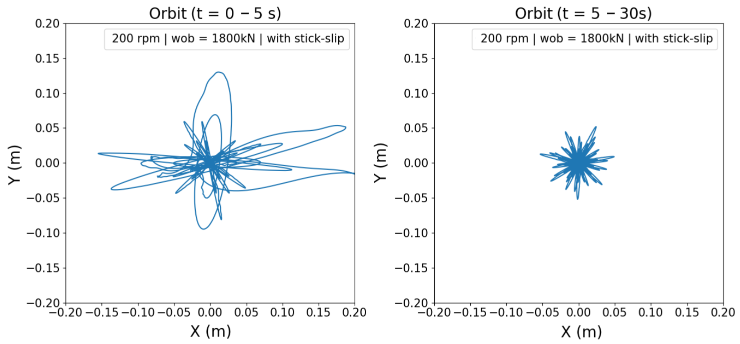

Figure 10. Orbit with *stick-slip* ($\Omega = 200rpm$)

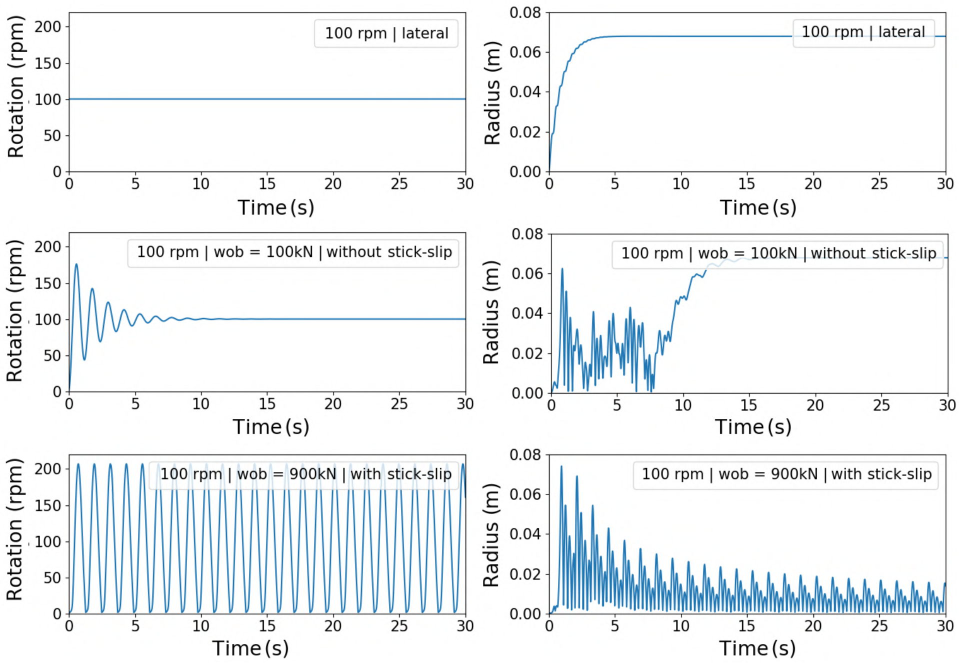

Figure 11. Influence of the coupling on radius time response ($\Omega = 100rpm$)

4. CONCLUSION

We have developed a low cost computational model capable of simultaneously simulating two of the main drilling vibration phenomena. However there are some aspects missing in the model, such as the fluid, and the impact between the string and the borehole.

When lateral e torsional formulation are coupled, in cases without stick-slip, the radius time responses have their transient regimes prolonged and with larger amplitudes, but in the permanent regime, the amplitude is the same as when there is no coupling. The scenery changes completely when there is stick-slip. Even with the amplitude dropping over time, the response oscillates permanently. At velocities close to natural frequency, the amplitudes are smaller, because

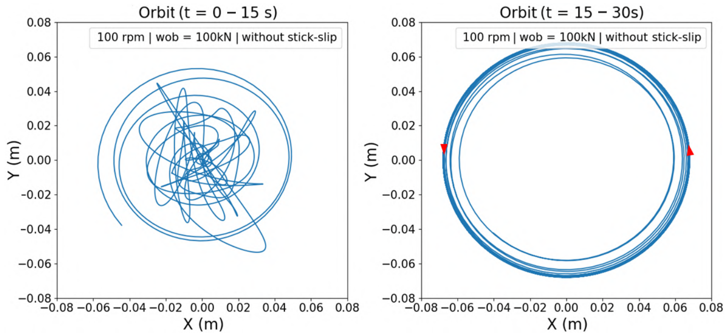

Figure 12. Orbit without *stick-slip* ($\Omega = 100rpm$)

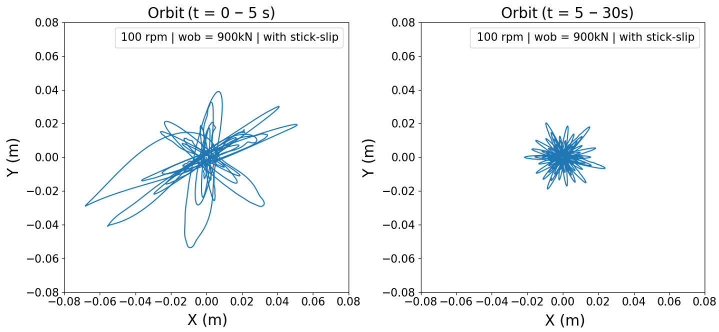

Figure 13. Orbit with *stick-slip* ($\Omega = 100rpm$)

the system does not resonate. In addition, for 50 rpm, we simulated a long time window and it was found that the system still does not reach the steady state after 1000s, but the amplitude is almost constant. As for the orbit, the inclusion of stick-slip totally changes its format, not assuming a circular trajectory anymore.

5. REFERENCES

Brett, J.F. *et al.*, 1992. "The genesis of bit-induced torsional drillstring vibrations". *SPE Drilling Engineering*, Vol. 7, No. 03, pp. 168–174.

Butlin, T. and Langley, R., 2015. "An efficient model of drillstring dynamics". *Journal of Sound and Vibration*, Vol. 356, pp. 100–123.

Cunha, J., 2002. "Effective prevention and mitigation of drilling problems". *World Oil & Gas Technologies*, Vol. 2, pp. 28–34.

Ishida, Y. and Yamamoto, T., 2013. *Linear And Nonlinear Rotordynamics: a modern treatment with applications*. John Wiley & Sons.

Jansen, J. *et al.*, 1992. "Whirl and chaotic motion of stabilized drill collars". *SPE Drilling Engineering*, Vol. 7, No. 02, pp. 107–114.

Jeffcott, H.H., 1919. "Xxvii. the lateral vibration of loaded shafts in the neighbourhood of a whirling speed.âĂŤthe effect of want of balance". *The London, Edinburgh, and Dublin Philosophical Magazine and Journal of Science*, Vol. 37, No. 219, pp. 304–314.

Kyllingstad, A., Halsey, G. *et al.*, 1987. "A study of slip-stick motion of the bit". In *SPE Annual Technical Conference and Exhibition*. Society of Petroleum Engineers.

Navarro-López, E.M. and Suárez, R., 2004. "Practical approach to modelling and controlling stick-slip oscillations in oilwell drillstrings". In *Proceedings of the 2004 IEEE International Conference on Control Applications, 2004*. IEEE, Vol. 2, pp. 1454–1460.

Ritto, T., Aguiar, R. and Hbaieb, S., 2017. "Validation of a drill string dynamical model and torsional stability". *Meccanica*, Vol. 52, No. 11-12, pp. 2959–2967.

Tucker, R. and Wang, C., 1997. "The excitation and control of torsional slip-stick in the presence of axial-vibrations". *Lancsos University*.

Wu, X., Karuppiah, V., Nagaraj, M., Partin, U.T., Machado, M., Franco, M., Duvvuru, H.K. *et al.*, 2012. "Identifying the root cause of drilling vibration and stick-slip enables fit-for-purpose solutions". In *IADC/SPE Drilling Conference and Exhibition*. Society of Petroleum Engineers.

6. RESPONSIBILITY NOTICE

The authors are the only responsible for the printed material included in this paper.